SUPPLEMENTAL INFORMATION

SUPPLEMENTAL MATERIAL AND METHODS

LC-MS\MS analysis of Msn2 gel bands

Coomassie-stained gel bands were washed with 50mM ammonium bicarbonate (ABC) and dried with acetonitrile (ACN). 200µL of 10mM dithiothreitol (DTT) was added and incubated for 30 min at 56°C to reduce disulfide bonds. DTT was washed off and cysteins were alkylated by incubation with 100µl of 54mM iodoacetamide (IAA) for 20 min at RT in the dark. Gel pieces were dried with ACN, then swollen in 10ng/µl trypsin (recombinant, proteomics grade, Roche) in 50mM ABC, pH 8.5 and incubated over night at 37°C. LysC-digests (Wako Chemicals GmbH) were incubated over night at 30°C. The reaction was stopped by adding formic acid to a final concentration of approximately 1% and peptides were extracted by sonication.

The peptides were separated on a reversed-phase-nano-HPLC (Ultimate, Switchos, Famos; Dionex, Thermo Fisher Scientific). Samples were applied to a trapping column (PepMap C18, 300µm × 5mm, Dionex) using 0.1% trifluoroacetic acid (TFA) (Pierce Biotechnology Inc) at a flow rate of 20µl/min. Bound peptides were eluted to a 75µm × 150mm analytical column of the same material (Dionex) at a flow rate of 250nl/min. Elution was performed by applying a linear gradient of 2.5-40% ACN in 0.1% formic acid in 3 hours. The HPLC was coupled online to a linear iontrap mass spectrometer (LTQ, Thermo Fisher Scientific), which was equipped with a nanoelectrospray ion source (Proxeon). The electrospray voltage at the distal coated silica nanospray capillaries of New Objective was set to 1500V. The mass spectrometer was operated in the data-dependent mode: each full scan (m/z 450-1600) was followed by MS/MS (MS2) scans of the four most abundant ions. MS/MS/MS (MS3) experiments were automatically triggered if a neutral loss of phosphoric acid (98, 49, 32.7Da for singly, doubly or triply charged precursor ions, respectively) was detected among the most intense 8 fragment ions in the preceding MS2 scan. The general settings of the LTQ were: ion transfer tube temperature 200°C; collision gas pressure 3.6 bar; automated gain control (AGC) target for full scan was set to 20000, for MS2 scans to 10000. Collision-induced dissociation (CID) settings were: normalized collision energy: 35%, activation value q: 0.25, activation time: 30ms, isolation width: +/- 4 Th.

The LysC digest was measured on an LTQ XL (Thermo Fisher Scientific) with CID and electron transfer dissociation (ETD) with the above defined instrument settings except

that precursors were selected for CID and subsequently for ETD (100ms activation time, 35% normalized collision energy, 0.250 activation Q).

The acquired spectra were processed with the Proteome Discoverer 1.3.0.339 software package (Thermo Fisher Scientific). The search was performed against a small protein database containing the sequences of keratins, proteolytic enzymes and a small selection of other proteins Precursor mass tolerance was set to 2Da, fragment tolerance to 0.8Da. Carbamidomethylation of Cys (+57Da) was set as a static modification, oxidation of Met (+16Da) and phosphorylation of Ser/Thr/Tyr (+80Da) as variable modifications. Three missed cleavages for trypsin (respect. 2 for LysC) were allowed. Results were filtered to a false discovery rate (FDR) of 1% on the peptide level by applying the XCorr values 1.6, 2.2, 3.32 for 1+, 2+, respect. 3+ -charged precursor ions on top ranked sequences.

The analysis of a LysC-digest on the QSTAR was performed as follows: The HPLC was directly coupled to a QSTAR pulsar i (AB SCIEX, Framingham, CA) hybrid mass spectrometer. The nanospray source from Proxeon (Thermo Fisher Scientific) was used as interface between HPLC and MS with the distal coated silica capillaries from New Objective. The electrospray voltage was set to 2100V. The mass spectrometer was operated in positive ionization mode; the TOF-MS scan was recorded in a window between 450 and 1400m/z. MS/MS spectra were acquired in the m/z region 50-1600Da. The instrument was externally calibrated with the CID fragment ions of a synthetic peptide (ALILTLVS). A TOF MS peptide spectrum was obtained first for 1 second and two ions with the highest intensity were fragmented afterwards. MS/MS spectra were accumulated for 2 seconds. Information dependent acquisition and enhanced mode was applied for the measurement. Fragmented ions were set onto a rejection list for 12 seconds. The collision energy was adjusted automatically according to the mass and charge state of the peptides.

Peak lists were generated by the Mascot script in Analyst QS. Peaks were not grouped, the spectra were centroided by Analyst QS. The mgf file was loaded for data base search into Discoverer 1.3 (Thermo Fisher Scientific). Sequest was used as search engine. Peptide tolerance was set to 2Da, fragment ion tolerance was set to 0.8Da. Carbamidomethylcysteine was set as static, oxidation of methionine residues, phosphorylation of serine, threonine and tyrosine residues as variable modifications. PhosphoRS 2.0 was used to evaluate phosphorylation sites and the spectra of possibly phosphorylated peptides were evaluated manually as well. An in-house generated FASTA data base was used for the search containing the sequences of the target proteins, common contaminants and proteolytic enzymes. Peptides were filtered according to the XCorr/charge state values, false positive rate was set to 5%.

LC-MS\MS analysis of Msn2 bead preparation

Beads were washed five times with 50mM ABC. Disulfide bonds were reduced with DTT (5% w/w of the estimated amount of protein) and cysteins were subsequently alkylated with IAA (25% w/w of the estimated amount of protein). DTT (25% w/w of the estimated amount of protein) was added to consume excess IAA and proteins were digested with trypsin (5% w/w of the estimated protein amount) at 37°C overnight. Digests were stopped by addition of TFA to approx. pH 3.

Tryptic peptides were separated on the UltiMateTM 3000 Dual LC System (Dionex). Peptides were loaded onto a precolumn (PepMAP C18, 0.3 × 5 mm, Dionex) and desalted for 40 min (flow rate 20 µl/min, 0.1% TFA). Peptides were eluted from the trapping column onto an analytical column (PepMAP C18, 75 µm × 150 mm, Dionex) with a flow rate of 275 nl/min and a gradient from 0% B to 100% B in 60 (or 90 min), followed by a washing step of 10 min with 10% B and 90% C (solvent A: 5% ACN 0.1 % formic acid, solvent B: 40 % ACN, 0.08 % formic acid, solvent C: 80% ACN, 10% trifluorethanol, 0.08% formic acid). The nano-HPLC was coupled online to a hybrid linear ion trap/Fourier transform ion cyclotron resonance mass spectrometer with a 7-T superconducting magnet (LTQ-FT, Thermo Fisher Scientific) via a nano-electrospray ionization source (Proxeon). Capillary temperature was set to 200°C and source voltage on metal-coated nano ESI emitters (New Objective) was 1.5 kV. The two detectors of the hybrid instrument were operated in parallel mode: during one full scan in the FT-ICR-cell (resolution 100.000, m/z 400-1800 Th) the five most abundant ions were subjected to MS/MS. Monoisotopic precursor selection was enabled. Neutral losses of 98, 49 and 32.6 in the MS2 triggered an MS3 analysis in the linear ion trap. Fragmented precursors were excluded from further fragmentation for 60 (respect. 120) sec (with 5ppm accuracy) and singly charged peptides were generally excluded from MS/MS analysis. Peptide identification and SILAC quantification were performed using the SEQUEST algorithm in the Proteome Discoverer 1.3.0.339 software package (Thermo Fisher Scientific). Carbamidomethylation of Cys was set as static modifications. Phosphorylation of Ser/Thr/Tyr, neutral loss of water from Ser/Thr, oxidation of Met and ^{13}C6 Lys/Arg were set as variable modifications. Spectra were searched against the SGD database (6717 entries, 03-Feb-2011) plus contaminants with tryptic specificity allowing 3 missed cleavages, a peptide tolerance of 3 ppm, a fragment ions tolerance of 0.8 Da. Quantitation settings were the default values for precursor ions quantifier, the event detector was set to 4 ppm. The results were filtered at the XCorr values to an FDR of 1% on the peptide level. The result lists were

combined in MS Excel and subjected to further data processing: for each SILAC experiment the mixing ratio was determined on the basis of the quantified unique peptides which contained no phosphorylation and no proline. Due to the metabolic Arg-Pro conversion the impact of heavy proline on the H:L ratios was determined: the divergence from a 1:1 ratio of unphosphorylated peptides containing 1 proline reflected the extent of $^{13}C_5$-Pro incorporation and was extrapolated for peptides containing more than 1 proline. The probability of phosphosite localization was calculated using the phosphoRS 2.0 software (7) implemented into Proteome Discoverer. A phosphosite probability of 75% or higher was considered as confidently localized. Results were divided in lists of highly confident localized (Supplemental Table ST1) and non-localized (< 75% probability) phosphosites (Supplemental Table ST2).Unphosphorylated peptides are listed in Supplemental Table ST3. Annotated MS/MS spectra were exported for all peptide-spectrum matches that mapped to Msn2. These data are available at http://www.proteomecommons.org/tranche under the project name "Yeast_Msn2_Phospho" and the password "YMR037C".

SRM analysis

Selected reaction monitoring (SRM) assays (10) were set up as following; The peptide mixture was separated on a reversed phase nano-HPLC (Ultimate 3000, Dionex). Peptides were concentrated and washed with 0.1% TFA on a trapping column (PepMap C18, 300µm×5mm, 3µm, 100Å) for 30 min at a flow rate of 25 µl/min. Bound peptides were eluted and separated on an analytical column (PepMap C18, 75µm×150mm, 3µm, 100Å) using a linear gradient from 2.5% to 40% ACN with 0.1% formic acid in 60 min at a flow rate of 300 nl/min. The HPLC was directly coupled to a TSQ Vantage triple quadrupole mass spectrometer (Thermo Fisher Scientific) via a nanoelectrospray ion source (Proxeon). The Q1 peak width of the instrument was set to 0.7 u. Synthetic peptides were used to select the most intense transitions and the optimal collision energies and to determine the retention time for the peptides of interest. An SRM method with 45 transitions (50ms dwell time each) containing transitions for the peptides of interest in phosphorylated and unphosphorylated form, as well as for two additional, unmodified peptides of Msn2 and a quantification peptide (AADITSLYK (9)) in the HTBeaq tag ((6) and Reiter *et al.*, manuscript submitted) for normalization purposes was set up. The Pinpoint 1.0 software (Thermo Fisher Scientific) was used for data analysis. For the time course experiments, a scheduled SRM method was set up with a cycle time of 2 seconds and the same list of 45 transitions. For a list of used transitions/CEs, see Supplemental Figure S3A. Fold over 0 minutes values of peak areas of

reference peptide transitions were calculated for each time point. The values were averaged and used for determination of loading differences (normalization factor). Fold over 0 minutes values of peak areas of transitions were individually averaged and corrected with the normalization factor to determine induction values from peptides of interest for each technical replicate. Induction values of the technical replicates were averaged for each peptide which resulted in the final fold over 0 minutes ratio. Induction values of the individual technical replicates were also used to determine geometric standard deviation. Results were multiplied with/divided by the geometric standard deviation to get the confidence interval (see Supplemental Table ST4).

SUPPLEMENTAL RESULTS

Cdc55 but not Rts1 is required for high level expression of hyperosmolarity stress-induced genes and sustained nuclear localization of Msn2

Deletion of *CDC55* leads to impaired expression of Msn2/4 target genes in response to hyperosmotic stress. This effect could either be caused by absence of the PP2A-Cdc55 complex or due to the enhanced activity of the remaining PP2A-Rts1 complex. In order to distinguish between these two possibilities we compared mRNA levels of *PGM2* in wild type, *cdc55*Δ, *rts1*Δ single and *cdc55*Δ*rts1*Δ double mutants in response to hyperosmotic stress (Supplemental Figure S1A). We obtained similarly reduced transcript levels in the double mutant and the *cdc55*Δ single mutant. However, we observed an enhanced level of the *PGM2* transcripts in the *rts1*Δ mutant compared to wild type. Furthermore, in the near-absence of PP2A activity (*pph21*Δ *pph22*Δ double deletion cells), expression of *PGM2* is severely impaired. These results excluded PP2A-Rts1 as a stress mediated transcriptional activator and strongly suggest a positive role for PP2A-Cdc55 in the regulation of stress-induced transcription.

To determine whether localization of Msn2 is also regulated by the PP2A subunit Rts1 we analyzed shuttling of an Msn2-GFP fusion protein in wild type, *cdc55*Δ, *rts1*Δ, and *cdc55*Δ*rts1*Δ strains. Expression of a DsRed fusion protein in the wild type allowed distinction from mutant cells. The fluorescence signal was recorded 10 minutes after exposure to 0.4M NaCl (Supplemental Figure S1B). Msn2 nuclear localization was strongly reduced in the *cdc55*Δ or the *cdc55*Δ*rts1*Δ mutant at this time point. Absence of Rts1 alone did not affect localization of Msn2-GFP, indicating that the Msn2 localization defect is due to loss of Cdc55 (Supplemental Figure S1B middle and right panel).

PP2A-Cdc55 regulates hyperosmotic stress response via an Msn2/4 specific mechanism

We studied Msn2/4 independent stress signaling pathways in the presence or absence of Cdc55. PP2A-Cdc55 could be selectively involved in the regulation of rapidly induced genes. The Cup2 (Ace1) dependent induction of the metallothionein gene *CUP1* displays fast and transient expression kinetics, similar to Msn2/4 dependent genes (8). We observed that expression dynamics after induction by 100µM $CuSO_4$ were similar in wild type and *cdc55*Δ mutant cells (Supplemental Figure S2A). Crz1 is a Calcineurin regulated transcription factor structurally related to Msn2/4 (5). mRNA levels of the Crz1 regulated gene *PCM1* were

rapidly induced after treatment with 200mM $CaCl_2$ in both wild type and *cdc55*Δ cells (Supplemental Figure S2B).

These observations strongly suggest that PP2A-Cdc55 influences Msn2/4 regulation but not other stress-induced transcription factors. Thus, we focused our attention on other aspects of Msn2 regulation and asked whether PP2A-Cdc55 influences the export machinery of Msn2. Msn2 and Msn4 require the exportin Msn5 for nuclear export. To test whether Msn5-dependent nuclear export requires PP2A-Cdc55 we tested localization of two other Msn5 regulated transcription factors. We found the nuclear accumulation of Crz1-GFP to be unchanged in response to elevated Ca^{2+} ion concentration in the *cdc55*Δ mutant. In addition, absence of Cdc55 did not influence the rapid nuclear export of a GFP-tagged version of Mig1 during acute glucose starvation (Supplemental Figures S2C and S2D). Thus, Msn5 regulated nuclear export is not generally influenced by PP2A-Cdc55, although it remains possible that PP2A-Cdc55 controls the Msn2-Msn5 interaction specifically.

PP2A-Cdc55 may directly influence the Msn2 phosphorylation pattern. The mediator subunit and protein kinase Srb10/Cdk8 has been shown to be of importance for Msn2 nuclear export and to directly phosphorylate Msn2 in response to heat stress (1). It has also been proposed to negatively regulate stress gene transcription (2). Therefore, we tested whether PP2A-Cdc55 antagonizes the Srb10 mediated regulation of Msn2. Transcript levels of *CTT1* and *HSP12* were analyzed in a set of strains lacking *CDC55*, *SRB10* or both genes. In accordance with earlier reports, we found higher levels of both transcripts in the *srb10*Δ mutant strain and severely impaired expression levels in *cdc55*Δ cells compared to wild type in response to hyperosmotic stress (Supplemental Figure S2E). If Srb10 and PP2A-Cdc55 regulate the same target sites (or if PP2A-Cdc55 regulates Srb10 activity), the transcription profiles of Msn2 dependent genes should be similar in both the *srb10*Δ mutant and *cdc55*Δ*srb10*Δ double mutant. However, we found that transcript levels of *CTT1* and *HSP12* were decreased in the *cdc55*Δ*srb10*Δ double mutant compared to the *srb10*Δ single mutant indicating that Cdc55 and Srb10 mediate Msn2 dependent transcriptional response via different substrates. The observed phenotype could result from enhanced nuclear localization of Msn2 in the *cdc55*Δ*srb10*Δ mutant. Therefore we determined the localization pattern of Msn2-GFP in all four strains in response to hyperosmolarity stress. We observed a similar localization pattern in wild type and *srb10*Δ cells. Interestingly, the *cdc55*Δ*srb10*Δ double mutant had a similar short nuclear accumulation of Msn2-GFP in response to hyperosmotic stress as the *cdc55*Δ single mutant (Supplemental Figure S2F). These results indicate that

regarding Msn2 regulation, the mediator subunit Srb10 functions most likely downstream of or in parallel to Cdc55.

SUPPLEMENTAL TABLE LEGENDS

Supplemental Table ST1: Confidently localized phosphorylation sites of Msn2. Msn2-phosphopeptides from all experiments (unstressed, hyperosmotic stress as well as glucose starvation) are listed. List shows phosphopeptides with a phosphorylation site probability of > 75% according to PhosphoRS 2.0.

Supplemental Table ST2: Non localized phosphorylation sites of Msn2. Msn2-phosphopeptides from all experiments with a phosphorylation site probability of <75% are listed.

Supplemental Table ST3: List of unphosphorylated peptides of Msn2 identified by mass spectrometry.

Supplemental Table ST4: Phosphorylation kinetics by SRM measurements. Peak areas of transitions (listed in Supplemental Figure S3) for S194, S201, S288, S304, S451 and S620 are listed. Stress induction ratios (blue) have been normalized with AQUA-peptide and two reference peptides of Msn2 (factor indicated in green). Time point 0 min has been set to 1.

Supplemental Table ST5: Microarray data sets corresponding to Figure 1.

Supplemental Table ST6: Tree View files corresponding to Figure 1.

Supplemental Table ST7: PKA site prediction analysis. Msn2 amino acid sequence was analyzed for putative PKA motifs. The following websites (status: October 2012) were used: http://mendel.imp.ac.at/sat/pkaPS/ (4), http://csbl.bmb.uga.edu/~ffzhou/gps_web/predict.php (11, 12) and http://kinasephos.mbc.nctu.edu.tw/ (3). Default settings were used except for the latter (prediction specificity was set to 95%).

SUPPLEMENTAL FIGURE LEGENDS

Supplementary Figure S1

Cdc55 but not Rts1 is required for a sustained response to hyperosmolarity stress

A) Wild type (W303), *cdc55*Δ, *rts1*Δ, c*dc55*Δ*rts1*Δ and *pph21*Δ*pph22*Δ mutant cells were grown to exponential phase and treated with 0.4M NaCl. mRNA levels of *PGM2* were determined by autoradiography. *IPP1 mRNA* levels were used as reference.

B) Stress induced nuclear localization of Msn2 is transient in *cdc55*Δ but not in *rts1*Δ mutant cells. Msn2-GFP (overexpressed from *ADH1* promoter) and ATPaseSu9-DsRed (only wild type) signals were recorded 10 minutes after exposure to hyperosmotic stress. Wild type cells were mixed with mutant cells directly before treatment.

C) Relationship between fold induction of full length Msn2 (X-axis) and Msn2ΔNES (Y-axis) genes.

D) Same as in (C) except that a *cdc55*Δ strain background was used.

E) Change of induction in wild type versus *cdc55*Δ determined for full length Msn2 (Y-axis) and Msn2ΔNES (X-axis).

F) Heat map of the figure 1 data set (163 induced genes) including the contrasts between genetic backgrounds at the indicated time points and contrasts of the respective untreated control. The right panel shows the corresponding values of the Msn2ΔNES (in *msn2Δmsn4Δ* background) experiment.

Raw data for (C), (D), (E) and for Treeview (F) are included in Supplemental Table ST5.

Supplementary Figure S2

Cdc55 does not affect Msn2 and Msn4 independent transcriptional stress responses, Msn5 dependent nuclear export and does not function upstream of the mediator subunit Srb10.

A) *CUP1* mRNA levels in wild type and *cdc55*Δ cells. Cells were treated with 100μM $CuSO_4$. Signals from two Northern blot hybridizations were quantified and averaged.

B) Time course of the mRNA levels of the Crz1-dependent gene *PCM1* in response to 200μM $CaCl_2$ in wild type and *cdc55*Δ cells.

C) Crz1-GFP localization in response to elevated Ca^{2+} levels is not dependent on Cdc55. Wild-type and *cdc55*Δ cells expressing Crz1-GFP under the control of its native promoter were grown to early logarithmic phase and treated with 200μM $CaCl_2$. Crz1-GFP

fluorescence was recorded from unfixed cells at the indicated time points. Representative images are shown.

D) Wild-type and *cdc55*Δ cells expressing Mig1-GFP were grown to early logarithmic phase and shifted to glucose free medium by washing. Mig1-GFP signal was recorded 3 minutes after removal of glucose.

E) Cdc55 does not regulate Srb10 activity towards Msn2. Logarithmic growing wild type, *cdc55*Δ, *srb10*Δ and *cdc55*Δ*srb10*Δ cells were treated with 0.4M NaCl. Expression levels of *CTT1* and *HSP12* mRNAs were determined on Northern blots.

F) Srb10 does not influence localization of Msn2-GFP. Localization of Msn2-GFP in unstressed cells and during hyperosmotic stress in *cdc55*Δ, *srb10*Δ and *cdc55*Δ/*srb10*Δ mutant cells.

G) RNA Pol II association to coding regions is shortened and reduced in *cdc55*Δ cells. Logarithmic growing *msn2/4*Δ and *msn2/4*Δ*cdc55*Δ cells carrying plasmid pMSN2Msn2ΔNES were treated with 0.4M NaCl followed by crosslinking with formaldehyde. ChIP of Rpb1 was performed as described in figure 3D. Binding of RNA Pol II to coding regions of *CTT1* and *HSP12* was quantified using multiplex PCR. Positions of the corresponding amplicons are indicated.

Supplementary Figure S3

SRM analysis of Msn2 phosphopetides.

A) List of peptides of Msn2 used in our SRM analysis. m/z values of precursor and single, double and triple charged N-terminal b-ions and C-terminal y-ions are indicated. CE: collision energy used for fragmentation. Synthetic peptides were used to select diagnostic transitions and the optimal collision energies and to determine the retention time for the peptides of interest. For reference peptides Ref-1 and Ref-2 diagnostic transitions were selected from CID spectra.

B) SRM analysis of the phosphorylation kinetics of Msn2 phospho-sites during hyperosmotic stress and glucose starvation. Levels of the unstressed sample (time point 0 minutes) were set to 1. Only results obtained with phosphopeptides are shown.

REFERENCES

1. **Chi, Y., M. J. Huddleston, X. Zhang, R. A. Young, R. S. Annan, S. A. Carr, and R. J. Deshaies.** 2001. Negative regulation of Gcn4 and Msn2 transcription factors by Srb10 cyclin-dependent kinase. Genes Dev **15:**1078-92.
2. **Holstege, F. C., E. G. Jennings, J. J. Wyrick, T. I. Lee, C. J. Hengartner, M. R. Green, T. R. Golub, E. S. Lander, and R. A. Young.** 1998. Dissecting the regulatory circuitry of a eukaryotic genome. Cell **95:**717-28.
3. **Huang, H. D., T. Y. Lee, S. W. Tzeng, and J. T. Horng.** 2005. KinasePhos: a web tool for identifying protein kinase-specific phosphorylation sites. Nucleic Acids Res **33:**W226-9.
4. **Neuberger, G., G. Schneider, and F. Eisenhaber.** 2007. pkaPS: prediction of protein kinase A phosphorylation sites with the simplified kinase-substrate binding model. Biol Direct **2:**1.
5. **Stathopoulos, A. M., and M. S. Cyert.** 1997. Calcineurin acts through the *CRZ1/TCN1*-encoded transcription factor to regulate gene expression in yeast. Genes Dev **11:**3432-44.
6. **Tagwerker, C., K. Flick, M. Cui, C. Guerrero, Y. Dou, B. Auer, P. Baldi, L. Huang, and P. Kaiser.** 2006. A tandem affinity tag for two-step purification under fully denaturing conditions: application in ubiquitin profiling and protein complex identification combined with in vivocross-linking. Mol Cell Proteomics **5:**737-48.
7. **Taus, T., T. Kocher, P. Pichler, C. Paschke, A. Schmidt, C. Henrich, and K. Mechtler.** 2011. Universal and confident phosphorylation site localization using phosphoRS. J Proteome Res **10:**5354-62.
8. **Thiele, D. J.** 1988. ACE1 regulates expression of the *Saccharomyces cerevisiae* metallothionein gene. Mol Cell Biol **8:**2745-52.
9. **Wepf, A., T. Glatter, A. Schmidt, R. Aebersold, and M. Gstaiger.** 2009. Quantitative interaction proteomics using mass spectrometry. Nat Methods **6:**203-5.
10. **Wolf-Yadlin, A., S. Hautaniemi, D. A. Lauffenburger, and F. M. White.** 2007. Multiple reaction monitoring for robust quantitative proteomic analysis of cellular signaling networks. Proc Natl Acad Sci U S A **104:**5860-5.
11. **Xue, Y., F. Zhou, M. Zhu, K. Ahmed, G. Chen, and X. Yao.** 2005. GPS: a comprehensive www server for phosphorylation sites prediction. Nucleic Acids Res **33:**W184-7.

12. **Zhou, F. F., Y. Xue, G. L. Chen, and X. Yao.** 2004. GPS: a novel group-based phosphorylation predicting and scoring method. Biochem Biophys Res Commun **325:**1443-8.

Figure S1

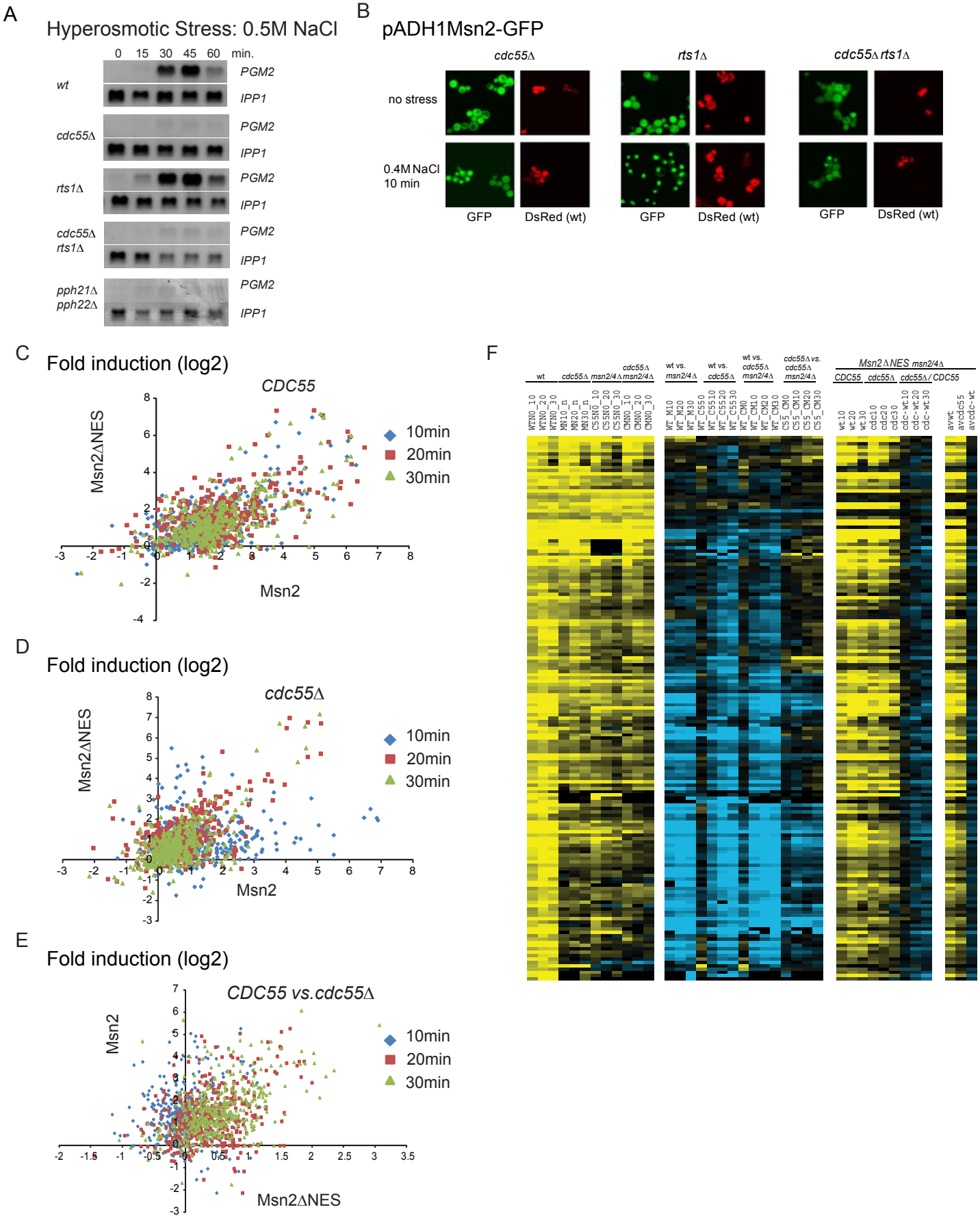
A
Hyperosmotic Stress: 0.5M NaCl
0 15 30 45 60 min.
wt
cdc55Δ
rts1Δ
cdc55Δ rts1Δ
pph21Δ pph22Δ
PGM2
IPP1
B
pADH1Msn2-GFP
cdc55Δ
rts1Δ
cdc55Δ rts1Δ
no stress
0.4M NaCl 10 min
GFP
DsRed (wt)
C
Fold induction (log2)
CDC55
Msn2ΔNES
Msn2
10min
20min
30min
D
Fold induction (log2)
cdc55Δ
Msn2ΔNES
Msn2
10min
20min
30min
E
Fold induction (log2)
CDC55 vs.cdc55Δ
Msn2
Msn2ΔNES
10min
20min
30min
F
wt
cdc55Δ
msn2/4Δ
cdc55Δ msn2/4Δ
wt vs. msn2/4Δ
wt vs. cdc55Δ
wt vs. cdc55Δ msn2/4Δ
cdc55Δ vs. cdc55Δ msn2/4Δ
Msn2ΔNES msn2/4Δ
CDC55
cdc55Δ
cdc55Δ/ CDC55

Figure S2

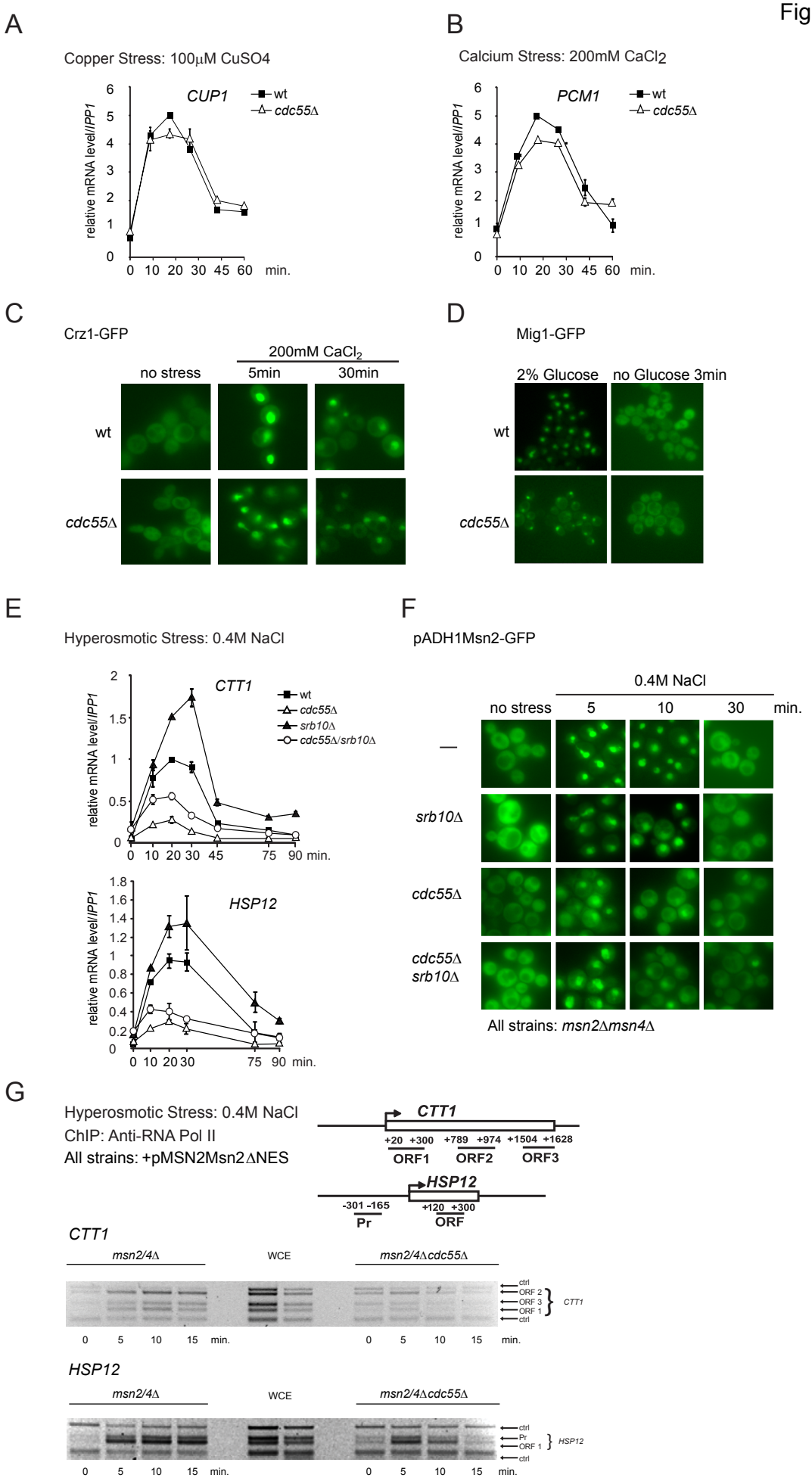
A
Copper Stress: 100μM CuSO4
CUP1
wt
cdc55Δ
relative mRNA level//PP1
0 10 20 30 45 60 min.
B
Calcium Stress: 200mM CaCl2
PCM1
wt
cdc55Δ
relative mRNA level//PP1
0 10 20 30 45 60 min.
C
Crz1-GFP
200mM CaCl2
no stress
5min
30min
wt
cdc55Δ
D
Mig1-GFP
2% Glucose
no Glucose 3min
wt
cdc55Δ
E
Hyperosmotic Stress: 0.4M NaCl
CTT1
wt
cdc55Δ
srb10Δ
cdc55Δ/srb10Δ
relative mRNA level//PP1
0 10 20 30 45 75 90 min.
HSP12
relative mRNA level//PP1
0 10 20 30 75 90 min.
F
pADH1Msn2-GFP
0.4M NaCl
no stress
5
10
30
min.
—
srb10Δ
cdc55Δ
cdc55Δ srb10Δ
All strains: msn2Δmsn4Δ
G
Hyperosmotic Stress: 0.4M NaCl
ChIP: Anti-RNA Pol II
All strains: +pMSN2Msn2ΔNES
CTT1
+20 +300
ORF1
+789 +974
ORF2
+1504 +1628
ORF3
HSP12
-301 -165
Pr
+120 +300
ORF
CTT1
msn2/4Δ
WCE
msn2/4Δcdc55Δ
ctrl
ORF 2
ORF 3
ORF 1
ctrl
CTT1
0 5 10 15 min.
0 5 10 15 min.
HSP12
msn2/4Δ
WCE
msn2/4Δcdc55Δ
ctrl
Pr
ORF 1
ctrl
HSP12
0 5 10 15 min.
0 5 10 15 min.

Figure S3

A Peptides used for SRM analysis

unphosphorylated peptides

Name	Sequence	precursor	transition	ion	charge	CE	syn-pep
AQUA	AADITSLYK	491,266			2+		yes
			611,339	y5	1+	20	
			724,423	y6	1+	20	
			839,45	y7	1+	20	
Ref-1	AGEGEIPAPLAGTVSK	748,901			2+		no
			772,456	y8	1+	28	
			940,546	y10	1+	28	
			1053,63	y11	1+	28	
Ref-2	INSPQQLQQQLNR	783,92			2+		no
			530,304	y4	1+	30	
			670,357	y11	2+	30	
			899,505	y7	1+	30	
			1027,56	y8	1+	30	
S194	AQQHTSIKDNR	649,334			2+		yes
			732,399	y6	1+	25	
			833,447	y7	1+	25	
			970,506	y8	1+	25	
			1009,51	b9	1+	25	
S201	LSLPNGANSNLFIDTNPNNLNEK	833,753			3+		yes
			414,714	y7	2+	23	
			942,463	y8	1+	24	
			1158,54	y10	1+	24	
S288	FSDVITNQFPSMTNSR	615,292			3+		yes
			396,687	y7	2+	15	
			792,366	y7	1+	18	
			939,435	y8	1+	18	
S304	NSISHSLDLWNHPK	549,946			3+		yes
			397,719	y6	2+	28	
			667,336	y11	2+	28	
			681,346	y5	1+	28	
S451	ASLPIIDDSLSYDLVNK	621,663			3+		yes
			751,398	y6	1+	15	
			796,414	y14	2+	14	
			838,43	y7	1+	16	
S451	ASLPIIDDSLSYDLVNK	931,99			2+		yes
			796,414	y14	2+	28	
			852,956	y15	2+	28	
			1268,6	y11	1+	27	
S633	RSSVVIESTK	553,314			2+		yes
			335,192	y3	1+	26	
			642,393	b6	1+	25	
			771,435	b7	1+	25	

phospho-peptides

Name	Sequence	precursor	transition	ion	charge	syn-pep	syn-pep
S#194	AQQHTS#IKDNR	689,317			2+		yes
			532,283	y4	1+	28	
			640,329	Reporter	2+	22	
			913,413	y7	1+	27	
S#304	NS#ISHSLDLWNHPK	576,601			3+		yes
			244,165	y2	1+	29	
			543,943	Reporter	3+	16	
			667,336	y11	2+	24	
			681,346	y5	1+	22	
			723,878	y12	2+	29	
S#633	RSS#VVIESTK	593,297			2+		yes
			464,235	y4	1+	23	
			544,309	Reporter	2+	23	
			676,387	y6	1+	23	
			775,455	y7	1+	23	
			851,402	b7	1+	23	

B SRM analysis of phospho-peptides